AJNR

Acute encephalopathy with bilateral thalamotegmental involvement in infants and children: imaging and pathology findings.

A Yagishita, I Nakano, T Ushioda, N Otsuki and A Hasegawa

AJNR Am J Neuroradiol 1995, 16 (3) 439-447
http://www.ajnr.org/content/16/3/439

Acute Encephalopathy with Bilateral Thalamotegmental Involvement in Infants and Children: Imaging and Pathology Findings

Akira Yagishita, Imaharu Nakano, Takakazu Ushioda, Noriyuki Otsuki, and Akio Hasegawa

PURPOSE: To investigate the imaging and pathologic characteristics of acute encephalopathy with bilateral thalamotegmental involvement in infants and children. **METHODS:** Five Japanese children ranging in age from 11 to 29 months were studied. We performed CT imaging in all patients, 10 MR examinations in four patients, and an autopsy in one patient. **RESULTS:** The encephalopathy affected the thalami, brain stem tegmenta, and cerebral and cerebellar white matter. The brain of the autopsied case showed fresh necrosis and brain edema without inflammatory cell infiltration. Petechiae and congestion were demonstrated mainly in the thalamus. CT and MR images showed symmetric focal lesions in the same areas in the early phase. These lesions became more demarcated and smaller in the intermediate phase. The ventricles and cortical sulci enlarged. MR images demonstrated T1 shortening in the thalami. The prognosis was generally poor; one patient died, three patients were left with severe sequelae, and only one patient improved. **CONCLUSIONS:** The encephalopathy might be a postviral or postinfectious brain disorder. T1 shortening in the thalami indicated the presence of petechiae.

Index terms: Brain, diseases; Brain, magnetic resonance; Infants, diseases

AJNR Am J Neuroradiol 16:439–447, March 1995

A strange type of acute encephalopathy has been reported in Japan (1–12). The acute encephalopathy occurs in infants and young children without sexual predilection and is preceded for several days by fever and symptoms of upper respiratory infection. These symptoms are followed by the rapid evolution of stupor and coma, associated with generalized seizures and decorticate and decerebrate rigidity without focal neurologic or meningeal signs. Although acute encephalopathy is similar to Reye syndrome, computed tomography (CT) images demonstrate symmetrical focal lesions in the thalami and brain stem tegmentum, frequently accompanied by abnormalities in the cerebral and cerebellar white matter. All patients in whom this condition has been diagnosed thus far have been Japanese infants and children, as far as we know. Here, we described the cranial magnetic resonance (MR) images of acute encephalopathy as compared with the pathologic findings in the brain of one autopsied case.

Methods

Five Japanese patients (four boys and one girl) were studied; age range was 11 months to 2 years, 5 months. No family history of acute encephalopathy was obtained. No patients had been recently immunized. All patients underwent CT examinations. During the first month of hospitalization, we performed CT examinations almost every week. Enhanced CT images with contrast medium were obtained from patients 3, 4, and 5. We performed 10 MR examinations in four of five patients. MR imaging was obtained by either a 1.5-T (patients 2 and 3) or a 0.5-T (patients 4 and 5) superconducting system. Spin-echo T1-weighted images (500–600/26/2 [repetition time/echo time/excitations] at 0.5 T, 500/15/4 at 1.5 T) and T2-weighted images (2000/100/2 at 0.5 T, 2500–3000/80–100/1 at 1.5 T) were obtained. The section thickness was usually 8 mm. Two patients (patients 2 and 3) underwent enhanced MR examinations with gadopentetate dimeglumine (0.1 mmol/kg).

Received June 24, 1994; accepted after revision September 26.

From the Department of Neuroradiology, Tokyo Metropolitan Neurological Hospital (A.Y.), Department of Neuropathology, Tokyo Metropolitan Institute for Neuroscience (I.N.), Department of Radiology, Oota General Hospital (T.U.), and Departments of Pediatrics (N.O.) and Pathology (A.H.), Odawara Municipal Hospital, Japan.

Address reprint requests A. Yagishita, MD, Department of Neuroradiology, Tokyo Metropolitan Neurological Hospital, 2-6-1, Masashidai, Fuchu, Tokyo 183 Japan.

AJNR 16:439–447, Mar 1995 0195-6108/95/1603–0439

TABLE 1: Clinical findings on admission

Patient	Age, mo	Sex	Fever	Vomiting	Convulsion	Consciousness Disturbance	SGOT*	Hyperammonemia	Protein Level in the CSF, mg/dL	CSF Pleocytosis	Glucose Level in the CSF, mg/dL
1	14	M	+	+	+	+	+	. . .	−	−	−
2	12	M	+	−	+	+	++	−	. . .	−	37
3	26	F	+	−	+	+	+	−	140	−	−
4	11	M	+	+	+	+	++	−	−	−	−
5	29	M	+	−	+	+	++	−	−	−	−

Note.—+ indicates positive; −, negative or normal; and CSF, cerebrospinal fluid.

*Serum glutamic oxaloacetic transaminase: −, 50 IU/L or less; +, 50–100 IU/L; ++, 100–300 IU/L.

We performed an autopsy in one case (patient 1). Brain specimens were stained with hematoxylin-eosin, Klüver-Barrera method for myelin sheaths, and Bodian method for silver staining.

Results

Clinical findings on admission and imaging findings at various stages are summarized in the Tables 1 and 2. Although stains and cultures of the cerebrospinal fluid and blood cultures were negative, fever and symptoms of upper respiratory infection preceded the neurologic symptoms in all of the patients. Serum influenza A virus titers were elevated in patients 4 and 5, but no virus titers were elevated in patients 1, 2, or 3. The prognosis was generally poor; patient 1 died, patients 3 and 4 remained in a vegetative state and in patient 5 spastic quadriplegia developed with relatively good cognitive abilities. Only patient 2 improved without sequelae. All patients received antipyretics for the preceding upper respiratory infection before the appearance of neurologic symptoms, but not aspirin. We performed no toxin screening tests.

CT images on admission (Fig 1) showed symmetrical areas of low attenuation in almost the whole thalami, pontine tegmenta, cerebellum, and periventricular white matter of all patients except patient 3. MR images of patient 2 at admission demonstrated abnormalities in the same areas as noted on CT images. All of these exhibited prolonged T2 and T1 relaxation times (Fig 2). Contrast-enhanced T1-weighted images showed abnormal enhancement only in the margin of the thalami (Fig 2). MR images of patient 3 on day 5 showed that the thalamic lesions exhibited short T1 (Fig 3) and long T2. All other lesions demonstrated prolonged T2 and T1. In the second through fourth week, the areas of low attenuation or abnormal signal intensity became more demarcated and smaller in all regions. However, the lateral and third ventricles and cortical sulci enlarged. Abnormal contrast enhancement was observed on CT images of only patient 5 on day 14 (Fig 4). In the intermediate and late phases, the lesions in the thalami of patients 2, 3, and 4 showed abnormal T1 shortening (Figs 2 and 3). Although the cortical sulci and ventricles remained enlarged in patients 3, 4, and 5, those of patient 2 enlarged less than in the previous examinations (Fig 2).

We performed an autopsy in patient 1. The autopsy was confined to the brain and a small piece of the liver. The unfixed brain was swollen with flattened sulci, but uncal or tonsillar herniation was not seen. Coronal sections of the formalin-fixed brain showed symmetric widespread softening with partial tissue dissolution in deep portions of the thalamus, cerebral hemispheres, brain stem tegmentum (Fig 1), and deep regions of the cerebellum. Histologically, all these areas consisted of fresh necrosis without proliferation of reactive astrocytes or microglial or inflammatory cell infiltration. Perivascular infiltrate of an amorphous serum-like substance was seen in the margin of the lesion in the thalami, cerebral white matter, and cerebellar white matter, but this was not observed at the core of the lesion. The thalamus demonstrated conspicuous rarefaction and poor staining of the neuropil (Fig 1), marked loss of neurons and glial cells, marked congestion of veins and capillaries, and frequent petechiae (Fig 1). In the mamillary bodies, there was no neuronal loss or pallor of staining (Fig 1). As far as the cerebral arteries available for microscopic examination were concerned, there was no obvious obstruction or other significant primary disease except wall necrosis within the lesion. Hepatocytes were laden with small lipid droplets without any obvious tendency for their nuclei to remain in the center.

TABLE 2: Imaging findings at various stages

Patient	Early Phase (days 1–7)	Intermediate Phase (days 8–30)	Late Phase (day 31–27 months)
1	CT (day 1): bilateral symmetric, low attenuation, pontine tegmenta, deep cerebellar hemispheres, thalami, external capsule, periventricular and deep white matter 3rd ventricle effaced		
2	MR (day 1): bilateral symmetric long T1, T2 pontine tegmenta, upper vermis, thalami, lenticular nuclei, periventricular white matter bilateral ringlike enhancement, thalami 3rd ventricle effaced CT (day 1): low attenuation, same areas as on MR images	MR (day 21): lesions decreased in size; short T1, mixed T2 thalami; long T1, T2 pontine tegmenta lesions in the upper vermis disappeared cortical sulci less enlarged	MR (day 42): lesions further decreased; short T1, mixed T2 thalami; long T1, T2 periventricular white matter; pontine abnormalities disappeared MR (day 75): long T1, T2 left thalami, short T1, long T2 right thalami cortical sulci and ventricle less enlarged MR (6 months): long T1, T2 left thalamus, short T1, long T2 right thalamus; cortical sulci less enlarged
3	CT (day 1): normal CT (day 4): bilateral symmetric, low attenuation, pontine tegmenta, deep cerebellar hemispheres, thalami, periventricular and deep white matter no enhancement MR (day 5): bilateral symmetric short T1, long T2 thalami; long T1, T2 pontine tegmenta, cerebellar and cerebral white matter no enhancement	CT (day 11): areas of low attenuation became smaller cortical sulci and ventricles enlarged	MR (day 40): short T1, mixed T2 thalami long T1, T2 pontine tegmenta, cerebellar and cerebral white matter all lesions decreased in size cortical sulci and ventricles enlarged
4	CT (day 1): bilateral symmetric, low attenuation, pontine and midbrain tegmenta, thalami, cerebellar and cerebral white matter no enhancement	CT (day 9): lesions with low attenuation became smaller coritcal sulci and ventricles enlarged	MR (day 45): short T1, long T2 thalami long T1, T2, pontine and midbrain tegmenta, periventricular white matter
5	CT (day 1): bilateral symmetric, low attenuation, pontine tegmenta, thalami, posterior lenticular nuclei, external capsule, deep cerebellar and cerebral white matter CT (day 4): nearly same lesions as on day 1 no enhancement	CT (day 14): patchy enhancement, thalami bilaterally, left posterior lenticular nucleus lesions with low attenuation became smaller cortical sulci and ventricles enlarged MR (day 30):* mixed T2, thalami long T2, pontine tegmenta, lenticular nuclei, cerebellar and cerebral white matter	MR (27 months): long T1, T2 thalami, pontine tegmenta, cerebellar and cerebral white matter

* T1-weighted images were not obtained.

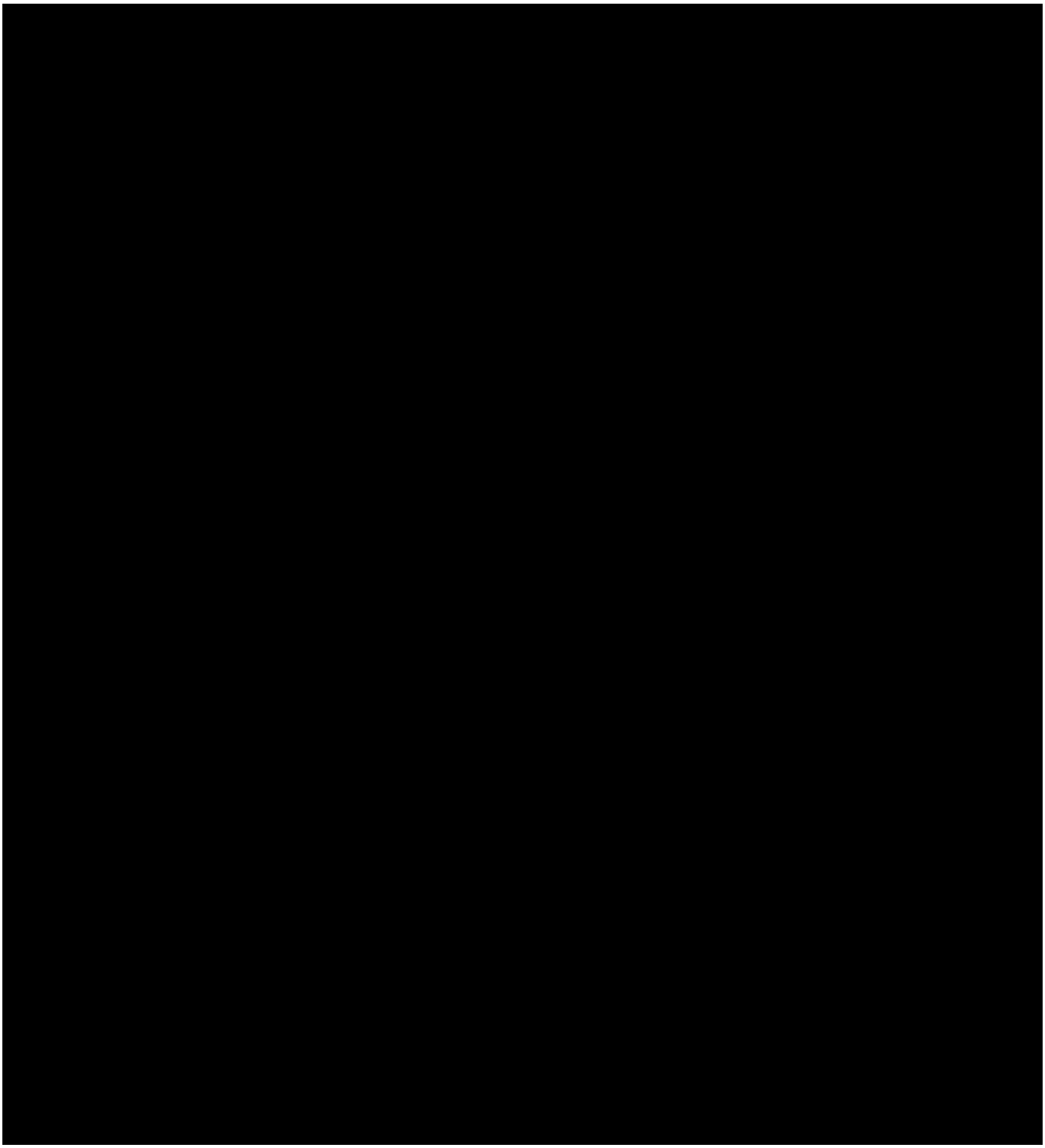

Fig 1. Patient 1. *A–C*, CT images at admission show bilateral symmetric areas of low attenuation in the pontine tegmentum, the deep portion of the cerebellar hemispheres (*A*), thalami, external capsule, periventricular white matter (*B*), and deep white matter (*C*). The temporal horn is enlarged. The third ventricle is effaced.

D, Coronal section of the formalin-fixed brain. Almost the whole thalamus on both sides demonstrates softening with brown discoloration and partial tissue dissolution, indicating symmetric necrotic lesions (*asterisk*). In addition, the white matter of the temporal lobe (*arrows*) and internal capsule (*arrowhead*) are involved with loss of normal white tint.

E, Almost the entire thalamus shows pallor (*asterisk*) with frequent petechiae (*arrowhead*). The hypothalamic portion including the mamillary body (*curved arrow*) is relatively preserved. The internal capsule (*I*) and parts of the cerebral white matter (*arrow*) are also pale. Myelin stain (Klüver-Barrera method), ×2. (*Continues.*)

Discussion

We found 26 patients with acute encephalopathy in previous reports including our five cases (1–12) (12 boys and 13 girls; age range, 6 to 96 months; mean age, 22.7 months). No family history of acute encephalopathy was obtained. No patients had been immunized just before the onset. Laboratory studies demonstrated an elevation of serum transaminases in all of the patients. However, hyperammonemia and hypoglycemia were rare. Cerebrospinal fluid pleocytosis was obtained in none of the patients. Serum influenza A virus titers were elevated in three patients, influenza B in one patient, measles virus in one patient.

Changes in the signal intensity in the thalami on MR images in patient 2 were consistent with the temporal evolution of hematomas (13–15). Furthermore, MR images of patients 3 and 4 showed areas of abnormal T1 shortening in the thalami. CT images of the thalami of these patients in the early phase showed no regions of hyperdensity suggesting hemorrhage or calcification. There have been two previous reports on brain pathology of patients with this encephalopathy who died during the early stage (2, 10) (personal communication from H. Ishihara). These studies reported almost identical pathologic findings as those of patient 1: fresh necrosis, brain edema in the margin of the lesions, and petechiae and congestion mainly in the thalamus. Thus, areas of short T1 in the thalami indicated the presence of methemoglobin in tiny hemorrhages, such as petechiae in the thalami of patient 1. Laminar necrosis and calcification are other postulated explanations for the T1 shortening (16), but these are unlikely in acute encephalopathy patients. Although subsequent studies suggested the presence of thalamic methemoglobin, initial MR scans did not reveal signal changes on T2-weighted images consistent with acute hemorrhage (deoxyhemoglobin). It is possible that the increased signal seen on initial T2-weighted images was caused primarily by edema, which may have obscured the presence of small petechial deoxyhemoglobin. There is a case report of acute encephalopathy in which MR images were described, including a description of lesions in the thalami with short T1 and long T2 on MR images on day 5, indicating methemoglobin in petechiae (12). These pathologic and imaging findings suggest the presence of petechiae in the thalami in acute encephalopathy.

Previous reports of acute encephalopathy demonstrated areas of low attenuation in the thalami on the first CT images after the appearance of neurologic symptoms (1–12). However, the CT images taken 4.5 hours after the convulsion of patient 3 were normal. CT images were taken after 12 hours or later in the other patients in the present study. Therefore, it was suggested that CT images might not show lesions in the very early phase of acute encephalopathy.

Patient 1 died and in patients 3, 4, and 5 severe sequelae developed. In contrast, patient 2 improved without sequelae. In this patient, the lesions in the cerebral white matter were smallest and enlargement of the cortical sulci and ventricles was reversible. Cerebellar and pontine abnormalities disappeared during the course of the illness. On the 21st day, administration of steroids and mannitol was terminated. This might be related to the reversible enlargement of the cortical sulci and ventricles.

CT images showing the same appearances as found in acute encephalopathy, excluding Japanese studies, were reported in Taiwan (17). This study reported three children with early onset of seizures and disturbed consciousness beginning after a few days of a nonspecific minor illness. The ages at the onset of disease were 9, 10, and 14 months. CT showed areas of low attenuation in the thalami bilaterally and in the periventricular regions. The lesions decreased in size on CT during the course of the disease. Brain stem lesions were not described. The authors of the report considered this condition to be acute encephalopathy caused by infarction of the whole thalamus. Whole tha-

Fig 1, *cont'd.*

F, Higher magnification of the thalamus demonstrates obvious vessel engorgement (*small arrow*) and frequent petechiae (*large arrow*) in addition to neuronal dissolution (*arrowhead*). Hematoxylin-eosin method, ×50.

G, The central portion of the frontal lobe including deeply located cortex (*N*) is markedly necrotic and pale. The deep white mater was predominantly involved (*asterisk*), but the digitated white matter was spared (*large arrows*). However, there was no tendency for U fibers (*arrowhead*) to be preserved. The border between the pale and well-stained white matter is sharp (*small arrow*). Myelin stain (Klüver-Barrera method), ×1.5.

H, The pontine tegmentum (*asterisk*) shows prominent pallor. Myelin stain (Klüver-Barrera method), ×4.7.

Fig 2. Sequential MR images in patient 2.

A, B, T2-weighted images (3000/100/1) on admission demonstrate bilateral symmetric hyperintense areas in the pontine tegmentum, upper vermis, thalami, and lenticular nuclei. The pontine base appeared markedly hypointense; however, the absolute signal intensity was nearly equal to that of the genu of the corpus callosum and anterior limb of the internal capsule. Therefore, we considered the pontine base normal.

C, The lesions in the thalami were hypointense on T1-weighted image (450/15/4). The third ventricle was effaced.

D, Enhanced T1-weighted image (450/15/4) demonstrated ringlike enhancement in the periphery of the thalami bilaterally (*arrow*).

E, On the 21st day, the lesions in the thalami were smaller and uniformly hyperintense relative to gray matter on T1-weighted image (450/15/4). The cortical sulci were enlarged. The third ventricle was visible.

F, Six months after onset, the size of the left thalamic lesion was further decreased and hypointense, whereas the right one was still hyperintense (*arrow*) on T1-weighted image (450/15/4). The cortical sulci were less enlarged.

lamic infarction on both sides without involvement of the ventral portion of the upper midbrain, however, is very unusual (18). We thought that these children had acute encephalopathy. To our knowledge, no patients with acute encephalopathy have been described in other countries.

The ascending reticular activating system, part of the brain stem reticular formation, is essential for maintaining normal cortical function (19). The system receives collateral from virtually all sensory pathways and projects to the midline and intralaminar nuclei of the thalamus, which in turn project diffusely to widespread cortical areas. Bilateral destruction of the midbrain reticular formation or of the midline and intralaminar nuclei of the thalamus causes coma (19). We suggest that coma in the patients might be caused by bilateral damage to these fibers in the thalami.

Viral encephalitis as a cause of acute encephalopathy was improbable because the cerebrospinal fluid in none of the patients showed pleocytosis. In addition, pathologic examinations of

Fig 3. T1-weighted image of patient 3 (500–600/15/2).

A, The image on the fifth day demonstrates symmetric central hyperintense lesions with peripheral hypointensity in the thalami (*arrow*).

B, The lesions in the thalami are smaller and uniformly hyperintense (*arrow*) on day 40. The cortical sulci and the ventricles were enlarged, indicating central volume loss.

the three brains with acute encephalopathy did not show any proliferation of reactive astrocytes or microglial or inflammatory cell infiltration. Acute toxic encephalopathy, Reye syndrome, and acute disseminated encephalomyelitis are postviral or postinfectious disorders (20–23). Acute toxic encephalopathy has been described as the most common postinfectious and postvaccinal brain disorder in children younger than 2 years old (21). In the pathology of the acute toxic encephalopathy, noninflammatory vascular changes (congestion and edema) predominate, and there is no demyelination (20, 21). Necrosis like that found in acute encephalopathy was not described in the acute toxic encephalopathy. Reye syndrome is an acute encephalopathy associated with fatty degeneration of the liver (24). The neuropathology of Reye syndrome is generally massive brain edema with only patchy, if any, necrosis, probably caused by circulatory disturbance from increased intracranial pressure (25, 26); the widespread symmetric necrosis like that seen in the three brains with acute encephalopathy has not been reported in the syndrome. Although the hepatic cells in patient 1 were laden with lipid droplets, fat appears in the liver whenever the body is under serious assault (27, 28). The combination of acute encephalopathy and hepatopathy is not unique to Reye syndrome (20). Hepatocytes in Reye syndrome show a uniform foaminess by fat droplets with central nuclei (22); on the other hand, hepatocytes in patient 1 were laden with small lipid droplets without any obvious tendency for their nuclei to remain in the center. Furthermore, brain imaging in Reye syn-

Fig 4. CT images of patient 5 after the administration of contrast medium.

A, The image on the fourth day demonstrates symmetric areas of low attenuation in the thalami, posterior lenticular nuclei, and external capsule on both sides. There is no abnormal enhancement.

B, The lesions are smaller and abnormal enhancement is visible in the thalami bilaterally and in the left posterior lenticular nucleus (*arrows*) on day 14.

drome generally shows diffuse brain edema with ventricular compression not unique as seen in acute encephalopathy (29, 30). In addition, the most characteristic and consistent biochemical abnormality in patients with Reye syndrome is hyperammonemia. The initial level of ammonia is believed to be directly related to the progression and severity of the symptoms (25). According to Corey, diagnostic criteria of Reye syndrome included hyperammonemia above 1.5 times the normal value (31). None of the patients with acute encephalopathy had hyperammonemia above 1.5 times the normal value. *Acute disseminated encephalomyelitis* is a collective term applied to a variety of severe, sometimes acutely fatal, infectious, inflammatory demyelinating diseases (32). It is known that the member diseases share an almost identical pathology consisting of multifocal, sometimes confluent, areas of inflammation that are usually exclusively perivenous and meningeal and accompanied by perivenous and subpial demyelination (32). The pathologic studies of the three brains of acute encephalopathy did not demonstrate demyelination or inflammatory cell infiltration. No patients had been recently immunized or vaccinated. Therefore, we considered acute disseminated encephalomyelitis unlikely as the cause of acute encephalopathy.

However, it has been reported that in postinfectious and postvaccinal disorders, a vasculopathy, which may be mild (a simple alteration of vessel wall permeability without anatomic disruption) or severe (vessel wall necrosis), is the first and probably a requisite phenomenon that initiates the reaction of the nervous tissue itself (20). Although this has almost always been ascribed to the venules, the arterioles and capillaries also may participate in producing this phenomenon. The immediate results of such involvement may include vascular occlusions leading to either encephalomalacia or focal lesions caused by venous stasis, transudation of serum with resulting perivascular and parenchymatous edema, diapedesis of red cells, and, in extreme cases, extensive perivascular and confluent hemorrhages, as well as migration of lymphocytes and plasma cells into perivascular spaces. Neuronal lesions may occur at this stage because of vascular insufficiency or occlusion, although they also may be triggered by a specific antigen-antibody reaction. It is yet unknown whether the vasculopathy leads to an inflammatory reaction or if the inflammatory reaction is a coincidental but independent phenomenon. Myelinoclasis may take place as a result of or at the same time as the vasculopathy, the edema, and the inflammatory reactions or as an independent phenomenon (20). Many factors, most of them yet unknown, determine the kind and extent of the tissue reaction. Thus, the reason one patient develops a congestive-edematous type of encephalopathy after smallpox vaccination, another has an acute hemorrhagic leukoencephalopathy, and yet another has the more classic disseminated perivenous myelinoclasis remains unexplained. The important point, however, is that the tissue reaction may vary considerably in type and severity or extent from individual to individual (20). Because acute encephalopathy was preceded by fever and symptoms of upper respiratory infection and occasionally serum virus titers were elevated and because pathologic findings of the three brains with acute encephalopathy showed necrosis, petechiae, and marked congestion of the veins and capillaries suggesting noninflammatory vascular changes, we considered that acute encephalopathy might be a postviral or postinfectious brain disorder, characterized by the presence of necrosis and petechiae and by the distribution of the lesions.

The possibility of cerebrovascular accident as the cause of this encephalopathy is slight; the necrotic lesions in the brain of patient 1 that were grossly symmetric and widespread do not correspond to the irrigation territory of any main cerebral artery (18, 33). Deep cerebral venous thrombosis can cause symmetric, diffuse thalamic infarcts (34); however, neither the brain of patient 1 nor MR images of the others showed venous thrombosis. Lesions with low attenuation in the cerebellar white matter and in the dorsal part of the brain stem also are observed on CT images in patients with maple syrup urine disease, but the clinical findings are different (35). Wernicke encephalopathy chiefly affects the mamillary bodies and periventricular regions around the third and fourth ventricles and aqueduct. The mamillary bodies, which are almost invariably affected in Wernicke encephalopathy (26), were left intact in this encephalopathy, indicating that acute encephalopathy differs from Wernicke encephalopathy.

In summary, in this study we investigated acute encephalopathy with bilateral thalamotegmental involvement in infants and children.

Pathologic findings were fresh necrosis, brain edema, petechiae, and congestion in the thalami, pontine tegmenta, and cerebral and cerebellar white matter. MR images of the brain are characteristic: symmetric lesions in the same areas as in the pathologic study, with T1 shortening in the thalami, indicating the presence of petechiae.

Acknowledgments

We thank Toshiro Nagai, MD, for his valuable comments during preparation of this report.

References

1. Aoki N, Kaneshi K, Mizuguchi M, et al. Computerized tomography in acute toxic encephalopathy: report of three cases with symmetrical low density areas in the thalami and the cerebellum (in Japanese). *No To Hattatsu* (Brain Develop) 1983;15:345–349
2. Hino T, Sai H, Morikawa Y, et al. A case of clinical Reye syndrome presenting characteristic CT changes (in Japanese). *No To Hattatsu* (Brain Develop) 1984;16:210–217
3. Inoue M, Sato K, Nomura T, et al. An autopsy case of Reye syndrome associated with Influenza B-virus infection and mimicking Leigh encephalopathy on brain CT (in Japanese). *Nihon Shounika Gakkai Zasshi* 1984;88:1429–1435
4. Aoki N. Acute toxic encephalopathy with symmetrical low density areas in the thalami and cerebellum. *Child Nerv Syst* 1985;1: 62–65
5. Mizuguchi M, Kamoshita S. Neuropathology of Reye syndrome (in Japanese). *Syounika Shinryou* 1986;49:1027–1035
6. Ochi J, Okuno T, Uenomiya Y, et al. Symmetrical low density areas in bilateral thalami in an infant with measles encephalitis. *Comput Radiol* 1986;10:137–139
7. Maeda K, Abe Y, Sasamoto A, et al. Three cases of acute encephalopathy with low density in thalamic regions on CT (in Japanese). *Shounika Rinsyo* 1987;40:99–104
8. Kiyonaga T, Kouno T, Shimoda K, et al. A case of acute encephalopathy presenting characteristic CT changes (in Japanese). *Shounika Rinsyo* 1988;41:92–96
9. Tateno A, Sakai K, Sakai S. Computed tomography of bilateral thalamic hypodensity in acute encephalopathy. *J Comput Assist Tomogr* 1988;12:637–639
10. Miura T, Umebara M, Oobu M. An autopsy case of acute encephalopathy with interesting CT findings (in Japanese). *Kitazato Igaku* 1989;19:460–462
11. Waki K, Kawamura M, Kidani K, Ishigame K. A case of acute encephalopathy with hypodensity of bilateral thalamus and cerebellum (in Japanese). *Shounika Rinsyo* 1989;42:1068–1072
12. Iai M, Tanabe Y, Goto M. Acute encephalopathy with symmetrical low density areas in the thalami on CT images: sequential changes of MR images and CT images (in Japanese). *No to Hattatsu* (Brain Develop) 1992;24:370–374
13. Gomori JM, Grossman RI, Goldberg HI, Zimmerman RA, Bilaniuk LT. Intracranial hematomas: imaging by high-field MR. *Radiology* 1985;157:87–93
14. Gomori JM, Grossman RI, Hackney DB. Variable appearance of subacute intracranial hematomas on high-field spin-echo MR. *AJNR Am J Neuroradiol* 1987;8:1019–1026
15. Thulborn KR, Atlas SW. Intracranial hemorrhage. In: Atlas SW, ed. *Magnetic Resonance Imaging of the Brain and Spine*. New York: Raven, 1991:175–222
16. Boyko OB, Burger PC, Shelburne JD, Ingram P. Non-heme mechanisms for T1 shortening: pathologic, CT, and MR elucidation. *AJNR Am J Neuroradiol* 1992;13:1439–1445
17. Wang HS, Huang SC. Infantile panthalamic infarct with a striking sonographic findings: the "bright thalamus." *Neuroradiology* 1993;35:92–96
18. Bewermeyer H, Dreesbach HA, Rackel A. Presentation of bilateral thalamic infarction on CT, MRI and PET. *Neuroradiology* 1985; 27:414–419
19. Nolte J. *The Human Brain*. 2nd ed. St Louis: CV Mosby, 1988: 359–363
20. Poser M. Diseases of the myelin sheath. In: Baker AB, Baker LH, eds. *Clinical Neurology*. Philadelphia: Harper & Row, 1978:90–95
21. Reik LJ. Immune-mediated central nervous system disorders in childhood viral infections. *Semin Neurol* 1982;2:106–114
22. Davis LE. Reye syndrome. In: Vinken PJ, Bruyn GW, Klawans HL, McKendall RR, eds. *Handbook of Clinical Neurology*. Vol 12 (56): *Viral Disease*. Amsterdam: Elsevier, 1989:149–177
23. Alvord EC. Disseminated encephalomyelitis: its variation in form and their relationships to other diseases of the nervous system. In: Vinken PJ, Bruyn GW, Klawans HL, Koetsier JC, eds. *Handbook of Clinical Neurology*. Vol 3 (47): *Demyelinating Diseases*. Amsterdam: Elsevier, 1985:467–502
24. Reye RDK, Morgan G, Baral J. Encephalopathy and fatty generation of the viscera: a disease entity in childhood. *Lancet* 1963; 2:749–752
25. Norenberg MD, Bruce-Gregorios J. Nervous system manifestations of systemic disease. In: Davis RL, Robertson DM, eds. *Textbook of Neuropathology*. 2nd ed. Baltimore: Williams & Wilkins, 1991:498–501
26. Duchen LW, Jacobs JM. Nutritional deficiencies and metabolic disorders. In: Adams JH, Duchen LW, eds. *Greenfield's Neuropathology*. 5th ed. New York: Oxford University Press, 1992:846–847, 813–817
27. Robins SL. *Pathology*. 3rd ed. Philadelphia: WB Saunders, 1957: 903–904
28. Bonnell HJ, Beckwith JB. Fatty liver in sudden death childhood death. *Am J Dis Child* 1986;140:30–33
29. Williams AL, Haughton VM. *Cranial Computed Tomography: A Comprehensive Text*. St Louis: CV Mosby, 1985:310–312
30. Wolpert SW, Barnes PD. *MRI in Pediatric Neuroradiology*. St Louis: CV Mosby, 1992:175
31. Corey L, Rubin JR, Bregman D, Gregg MB. Diagnostic criteria for influenza B associated Reye syndrome: clinical vs. pathologic criteria. *Pediatrics* 1977;60:702–708
32. Raine CS. Demyelinating diseases. In: Davis RL, Robertson DM, eds. *Textbook of Neuropathology*. 2nd ed. Baltimore: Williams & Wilkins, 1991:535–620
33. Takahashi S, Goto K, Fukasawa H, Kawata Y, Uemura K, Yaguchi K. Computed tomography of cerebral infarction along the distribution of the basal perforating arteries, II: thalamic arterial group. *Radiology* 1985;155:119–130
34. Eick JJ, Miller KD, Bell KA. Computed tomography of deep cerebral venous thrombosis in children. *Radiology* 1981;140: 399–402
35. Brismar J, Aqeel A, Brismar G, Coates R, Gascon G, Ozand P. Maple syrup urine disease: findings on CT and MR scans of the brain in 10 infants. *AJNR Am J Neuroradiol* 1990;11:1219–1228

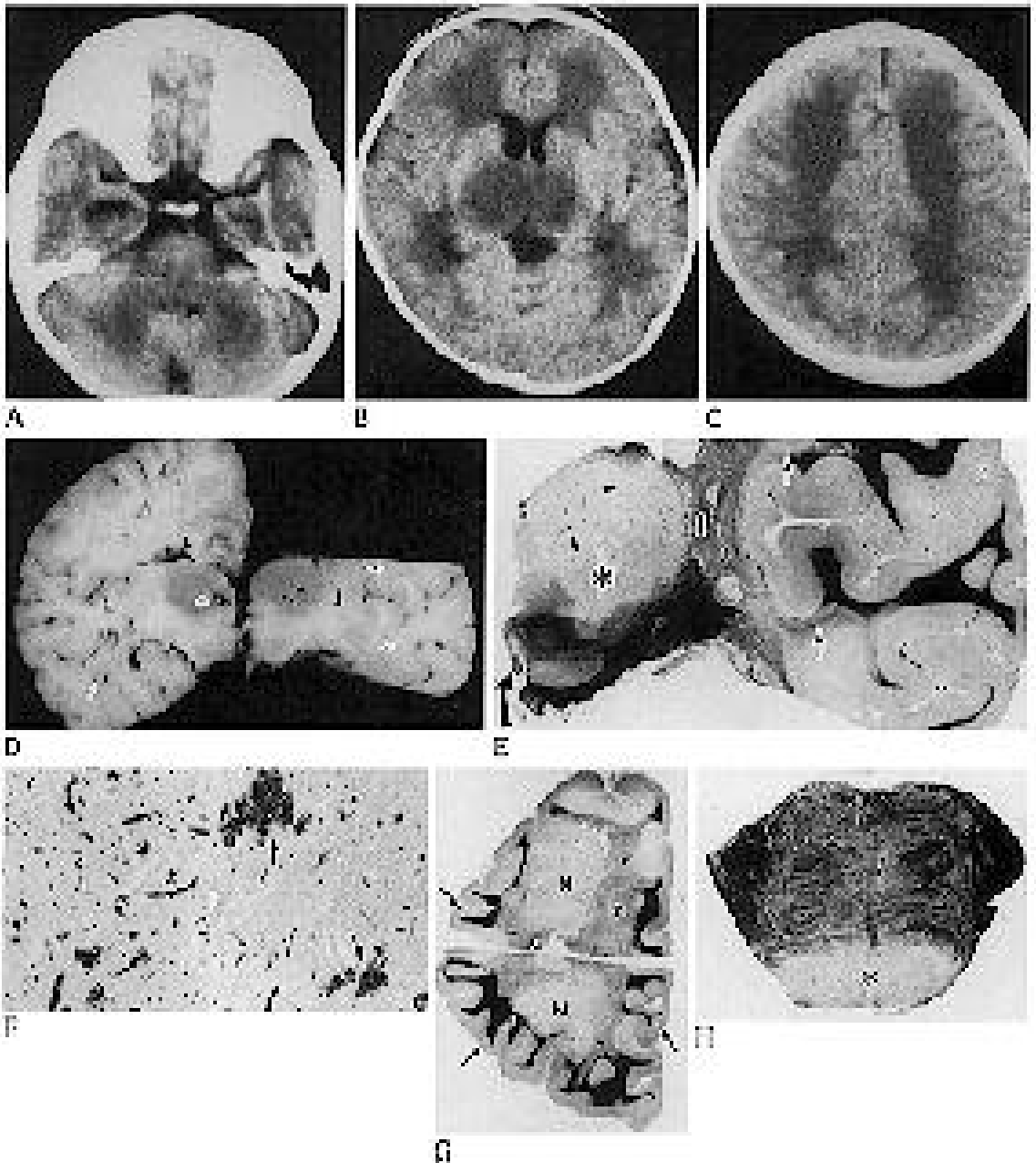
A
B
C
D
E
F
G
H

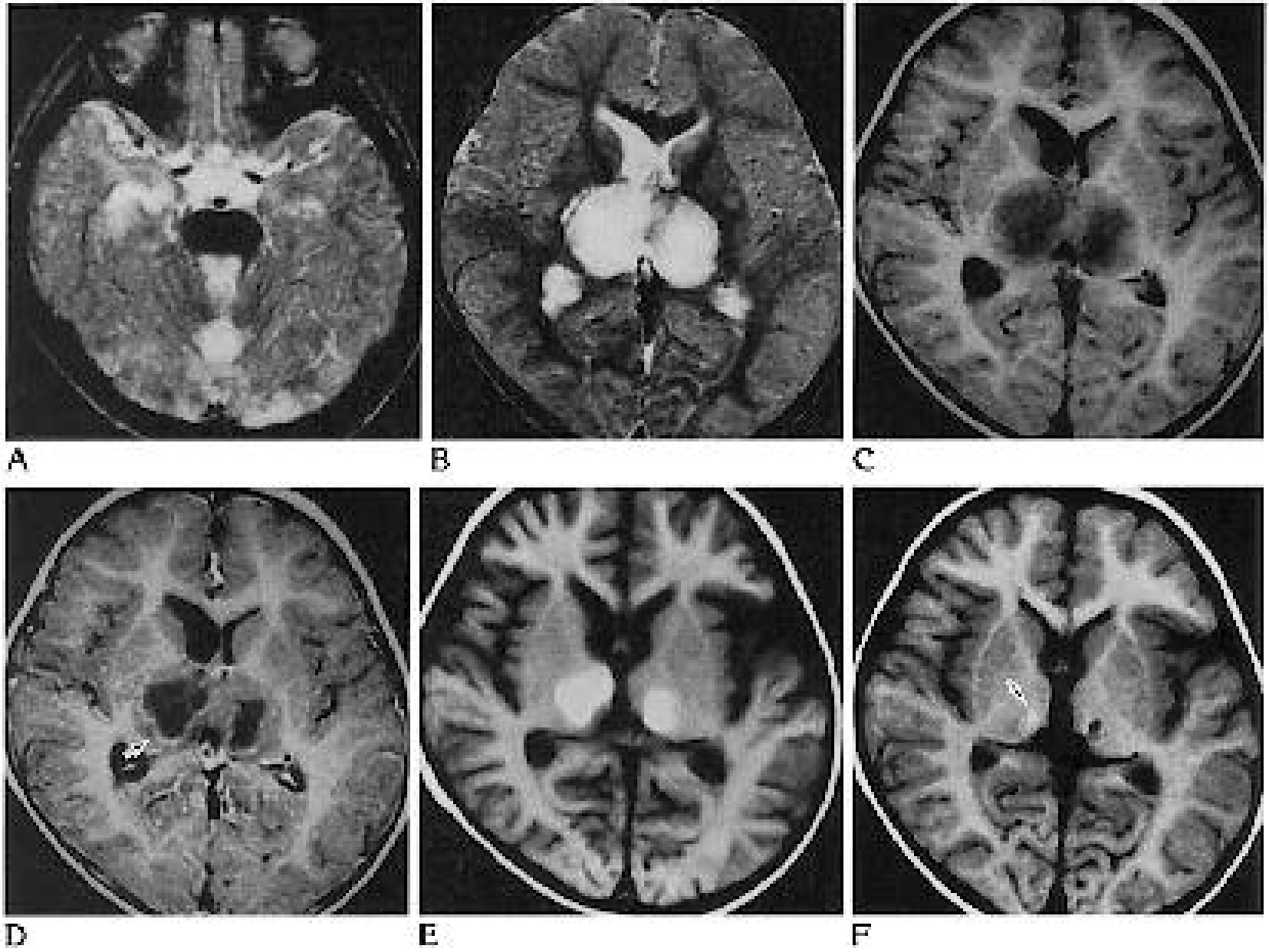
A
B
C
D
E
F

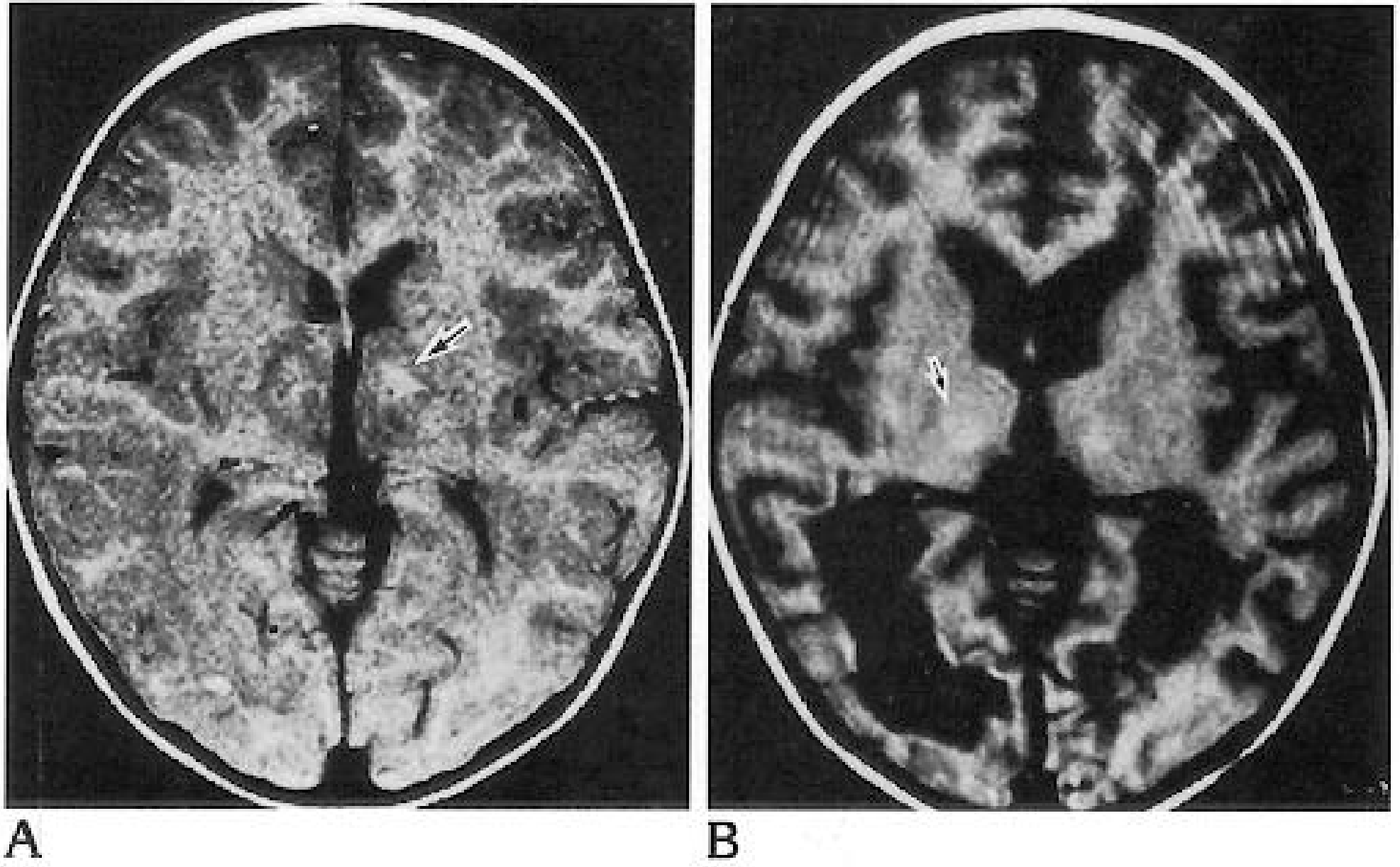
A
B

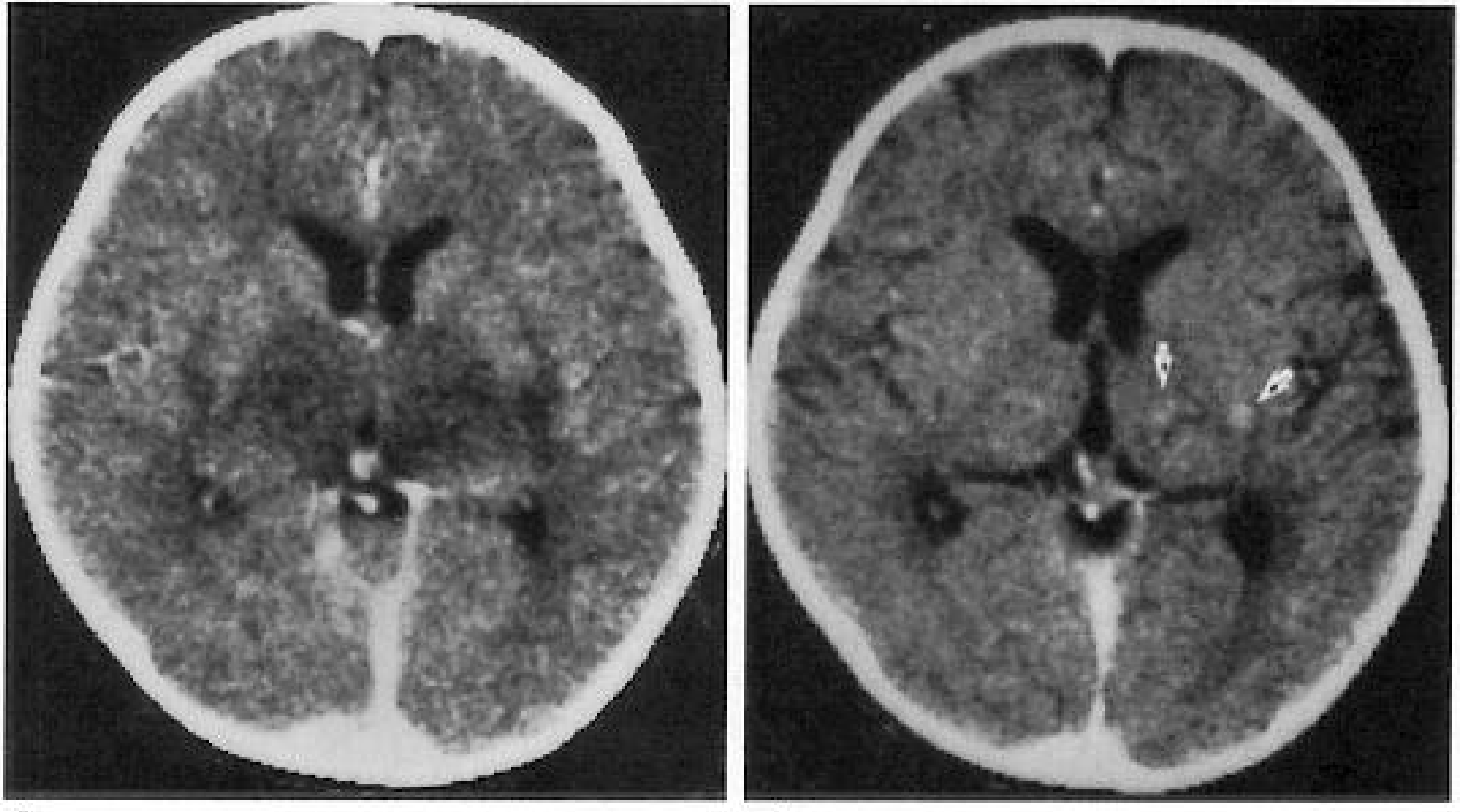
A
B